

Why even is odd: spin-orbit coupling and strong electronic correlations in cyclic molecules

A. L. Khosla,^{1,*} A. C. Jacko,¹ J. Merino,² and B. J. Powell¹

¹*School of Mathematics and Physics, The University of Queensland, Queensland, 4072, Australia*

²*Departamento de Física Teórica de la Materia Condensada,
Condensed Matter Physics Center (IFIMAC) and Instituto Nicolás Cabrera,
Universidad Autónoma de Madrid, Madrid 28049, Spain*

In atoms spin-orbit coupling (SOC) cannot raise the angular momentum above a maximum value or lower it below a minimum. Here we show that this need not be the case in materials built from ‘artificial atoms’, e.g., multi-nuclear coordination complexes or nanostructures. We demonstrate that in cyclic molecules the electronic spin couples to currents running around cyclic molecules. For odd membered rings the SOC is highly analogous to the atomic case; but for even membered rings every angular momentum state can be both raised and lowered. These differences arise because for odd membered rings the maximum and minimum molecular orbital angular momentum states are time reversal conjugates, whereas for even membered rings they are aliases of the same single state. We show, from first principles calculations, that this molecular SOC is large in suitable molecules. Finally, we show that when electronic correlations are strong molecular SOC can cause highly anisotropic exchange interactions and discuss how this can lead to effective spin models with compass Hamiltonians.

I. INTRODUCTION

Electrons traveling at relativistic velocities experience a spin-orbit coupling (SOC): $H_{\text{SO}} = \mathbf{K} \cdot \boldsymbol{\sigma}$, where $\boldsymbol{\sigma}$ is the spin operator. The properties of the pseudovector \mathbf{K} depend on the symmetry of the system. For spherical symmetry, e.g., in atoms, $\mathbf{K} = \lambda \mathbf{L}$, where λ is a constant and \mathbf{L} is the orbital angular momentum. But in lower symmetry environments SOC can be rather different. Important instances of this were discovered by Dresselhaus and Rashba [1, 2].

In spherically symmetric systems there is an maximum (minimum) state that cannot be surpassed by applying a raising (lowering) angular momentum operator. This constrains which states are coupled by SOC [3]. However, we will see below, that in systems built from ‘artificial atoms’ it is possible to modify these constraints and realize different spin-orbit Hamiltonians. Such artificial atoms could be realized as multi-nuclear coordination complexes [4–6], and these are the systems we will primarily explore as they are the most mature platform for our ideas, but our results apply equally to any other system with the same symmetry, for example, arrays of heavy atoms arranged into polygons on a surface. In principle, materials built from artificial atoms would also allow the engineering of specific SOC Hamiltonians tuned to different applications.

In this paper, we demonstrate that in cyclic molecules the electronic spin couples to currents running around the ring. For odd membered rings the spin molecular-orbital coupling (SMOC) is highly analogous to the atomic SOC; but for even sided rings every angular momentum state can be both raised and lowered. We present density den-

sity functional calculations that identify specific multi-nuclear organometallic complexes where the SMOC is large compared to other relevant energy scales. Finally, we explore a potential application of our findings: controlling the anisotropy of magnetic exchange interactions in systems where electronic correlations are strong. We show that the interplay of SMOC with electronic correlations can give rise to effective spin models with compass Hamiltonians. These models are known to give rise to many interesting states of matter, including some with topological order. Unlike previous schemes to realize such Hamiltonians, these effects do not rely on hopping through intermediate atoms or molecules.

Potential applications of designer SOC range from spintronics to more efficient lighting [1, 2, 7]. Furthermore, strong SOC is required to realize many symmetry projected topological phases of matter, such as topological insulators and superconductors, quantum spin Hall states, axion insulators and Weyl semimetals [8–12].

When both SOC and electronic correlations are strong even additional phases are possible, including topological Mott and Kondo insulators [13, 14]. Moreover, these ingredients allow for true topological order, which is characterized by long range-entanglement and often supports fractionalized quasiparticles [15, 16]. Interest in this physics was redoubled by Kitaev’s exact solution [17] of a compass model, *i.e.*, a spin model with exchange interactions that are highly anisotropic in both real- and spin-space [18]. Kitaev found a topological spin liquid with non-abelian anyonic excitations, which is sufficient to enable fault tolerant quantum computation [19]. Jackeli and Khaliullin [20] argued that the low-energy physics of a class of iridium-oxides (iridates) are described by the Kitaev model because of their strong SOC. However, it was soon realized that in this picture there must be a large isotropic exchange interaction [21]. More recently, it has been argued that the Kitaev model does not de-

*Electronic address: amie.khosla@uqconnect.edu.au

scribe the iridates [22]. This has renewed the search for materials that may realize the physics of the Kitaev and other compass models [23, 24]. However, in previous proposals the SOC arises from intra-atomic SOC on a transition metal, which is surrounded by multiple light atoms, thus the SOC is essentially atomic [25].

In molecular crystals the electrons hop between molecular orbitals which are significantly larger than the atomic orbitals relevant in, say, transition metal oxides. This leads to an effective on-site Coulomb interaction, U , that is typically an order of magnitude smaller than in transition metal oxides [26, 27]. However, the intramolecular hopping integral, t , is also typically an order of magnitude smaller. This means that electrons in molecular crystals are typically strongly correlated. Furthermore, this implies that the relative strength of SOC can be large in molecular crystals.

In organic materials the largest contributions to SOC typically arise from sulfur or selenium atoms [28]. Therefore, a powerful strategy for increasing SOC is to move to organometallic complexes; this has driven much recent progress in organic solar cells and organic light-emitting diodes [7]. Therefore, multi-nuclear organometallic complexes (i.e., molecules containing multiple transition metal atoms) with ligands that facilitate effective charge transport between molecules [4–6] provide a platform to serve as artificial atoms that will allow synthetic control and engineering of SOC beyond the possibilities available in inorganic systems. Furthermore, these materials will facilitate new ways to explore the interplay of the SOC with strong electronic correlations. Thus, we propose that compass models can be realized by using multi-nuclear organometallic complexes as artificial atoms.

II. SPIN-ORBIT HAMILTONIAN IN CYCLIC MOLECULES

In the Pauli equation [29] (the simplest low velocity approximation to the Dirac equation)

$$\mathbf{K} = \frac{\hbar}{4m^2c^2}(\mathbf{p} \times \nabla V(r)) \quad (1)$$

where $V(r)$ is the potential in which the electrons move and \mathbf{p} ($\boldsymbol{\sigma}$) is the momentum (spin) operator. The standard approaches to this problem in molecular systems are either to evaluate from first principles [7, 28] or to assume that only the SOC on selected heavy atoms is relevant and the SOC retains the spherical symmetry of the atomic case [7, 20, 21, 30, 31]. Here we take the alternative approach of simply analyzing which matrix elements are allowed in arbitrary molecules with cyclic, C_N , symmetries. This analysis will make extensive use of the cyclic double groups \tilde{C}_N , Table I.

It is convenient to introduce an orthogonal set of single electron basis states. The μ th basis state in the fermionic representation $\bar{\Gamma}_j$ can be written as $|\bar{j}_\mu\rangle = |\underline{k}_\nu; \sigma\rangle \equiv$

Odd N	E	$(C_N)^n$	\bar{E}	$(\bar{C}_N)^n$	TR
A_0	1	1	1	1	$\mathcal{T} 0\rangle = 0\rangle$
E_k	1	ω^{kn}	1	ω^{kn}	$\mathcal{T} k\rangle = (-1)^k -k\rangle$
E_j	1	ω^{jn}	-1	$-\omega^{jn}$	$\mathcal{T} j\rangle = (-1)^{j-\frac{1}{2}} -j\rangle$
$A_{N/2}$	1	$(-1)^n$	-1	$(-1)^{n-1}$	$\mathcal{T} N/2\rangle = N/2\rangle$
Even N	E	$(C_N)^n$	\bar{E}	$(\bar{C}_N)^n$	TR
A_0	1	1	1	1	$\mathcal{T} 0\rangle = 0\rangle$
E_k	1	ω^{kn}	1	ω^{kn}	$\mathcal{T} k\rangle = (-1)^k -k\rangle$
$B_{N/2}$	1	-1	1	-1	$\mathcal{T} N/2\rangle = N/2\rangle$
E_j	1	ω^{jn}	-1	$-\omega^{jn}$	$\mathcal{T} j\rangle = (-1)^{j-\frac{1}{2}} -j\rangle$

TABLE I: Character tables [32, 33] for the double groups \tilde{C}_N . For a given N , representations ‘above the line’ describe bosonic states (including even numbers of fermions), while those below the line are fermionic representations. The names of the representations, A , B and E , are chosen in accordance with Schoenflies notation. The additional subscript denotes angular momentum about the C_N axis associated with the states that transform according to the representation. The operations of the single group are the identity, E , and rotation by $2\pi n/N$, $(C_N)^n$. The additional operations of the double group are indicated by a bar above these operations, implying a further rotation by 2π . Group multiplication simply adds the subscripts with periodic boundary conditions such that the sum lies in the interval $(-N/2, N/2]$. The rightmost column indicates the behavior of a typical state that transforms according to the given representation under time reversal. For $N \geq 3$ S^z , S^+ , and S^- are bases of A_0 , E_1 , and E_{-1} respectively. Here $1 \leq n \leq N-1$ and $\omega = \exp(i2\pi/N)$. For odd N , $(1-N)/2 \leq k \leq (N-1)/2$ and $-\frac{N}{2} < j \leq \frac{N}{2}$. For even N , $-\frac{N}{2} < k \leq \frac{N}{2}$ and $(1-N)/2 \leq j \leq (N-1)/2$. k is integral and j is half-odd-integral for all N . $k=0$ refers to the representation A_0 and $j=N/2$ ($k=N/2$) refers to $A_{N/2}$ ($B_{N/2}$).

$|\underline{k}_\nu\rangle \otimes |\sigma\rangle$, where the molecular orbital part of the wavefunction, $|\underline{k}_\nu\rangle$, is the ν th basis state that transforms as $\underline{\Gamma}_k$, a bosonic representation with integer k , and the spin part, $|\sigma\rangle$, transforms as $|\uparrow\rangle \in E_{1/2}$ and $|\downarrow\rangle \in E_{-1/2}$ for the non-trivial cyclic groups.

SMOC obeys a set of selection rules, which are derived in Appendix A: (1) SMOC does not couple time reversed states:

$$\langle \bar{j}_\mu | H_{\text{SO}} \mathcal{T} | \bar{j}_\mu \rangle = 0, \quad (2a)$$

where \mathcal{T} is the time reversal operator. This is a corollary to Kramers’ theorem [33]. (2) States with the same spin are only coupled by SMOC if their orbital parts belong to the same irreducible representation:

$$\langle \underline{k}_\mu; \sigma | H_{\text{SO}} | \underline{q}_\nu; \sigma \rangle = \sigma \lambda_{k;\mu\nu}^z \delta_{kq}, \quad (2b)$$

where $\lambda_{k;\mu\nu}^z = \lambda_{k;\nu\mu}^{z*} = -\lambda_{-k;\mu\nu}^z$ is a constant and $\sigma = \pm 1/2$. (3) States with opposite spins are only coupled by SMOC if this conserves $j = k + \sigma$:

$$\langle \underline{q}_\nu; -\sigma | H_{\text{SO}} | \underline{k}_\mu; \sigma \rangle = \frac{1}{2} \lambda_{k+\sigma;\mu\nu}^\pm \delta_{k,q-2\sigma}, \quad (2c)$$

where $\lambda_{k+\frac{1}{2};\mu\nu}^\pm$ is a constant. Note that these selection rules are quite natural if one interprets k as the molecular angular momentum about the C_N axis, henceforth the z -axis, and j as the total angular momentum about z .

As Eqs. (2) only depend on the symmetries of the Pauli Hamiltonian other low-velocity approximations to the Dirac equation [29] yield the same selection rules. Furthermore, Eqs. (2) can be derived from, e.g., the Briet-Pauli formalism if the two-electron SOC is treated at the mean-field level [34, 35].

These selection rules have surprising consequences in cyclic molecules. To illustrate this, we consider the simplest class of models, where the low-energy physics is described by N orbitals related by the cyclic symmetry described by the group C_N , e.g., the one-band tight-binding, Hubbard, and t - J models. The assumption that only a single orbital is relevant to each heavy atom is natural for the transition metals in multi-nuclear organometallic complexes. Typically, in such molecules the transition metals sit in low-symmetry environments, thus often the degeneracy of the atomic d -orbitals will be completely lifted.

The \tilde{C}_N tight-binding model is diagonalized by a Bloch transformation. However, $\mathcal{T}^{-1}S^\pm\mathcal{T} = -S^\mp$ and H_{SO} is time-reversal symmetric; implying that $\mathcal{T}^{-1}K^\pm\mathcal{T} = -K^\mp$, where $K^\pm \equiv K^x \pm iK^y$. To avoid phase factors in the operators it is convenient to absorb them into the basis states:

$$|k\rangle = \eta_k \sum_r e^{i\phi kr} |r\rangle, \quad (3)$$

where $-N/2 < k \leq N/2$ and $0 \leq r \leq N-1$ are integers, $|r\rangle$ is a Wannier orbital centered at r , $\phi = 2\pi/N$ and η_k is a phase factor. For SO(3) symmetry the η_k are usually chosen following the Condon-Shortley convention, $\eta_k = i^{|k|}$, cf. e.g., the spherical harmonics. However, this does not respect time reversal symmetry for ‘aromatic’ systems, where $N = 4n + 2$ for integer n . Therefore, we set $\eta_k = i^{|k|}$, which introduces the required phases for arbitrary N . The state $|k\rangle$ is a basis for Γ_k and describes a (spinless) fermionic current running around the molecule with angular momentum $\hbar k$.

Applying the selection rules [Eqs. (2)], one finds that for odd N

$$H_{\text{SO}} = \sum_{m=1}^L \sum_{\sigma=-1/2}^{1/2} \sigma \lambda_m^z \left(\hat{c}_{m\sigma}^\dagger \hat{c}_{m\sigma} - \hat{c}_{-m\sigma}^\dagger \hat{c}_{-m\sigma} \right) + \frac{1}{2} \sum_{j=\frac{1}{2}}^{L-\frac{1}{2}} \left[\lambda_j^\pm \left(\hat{c}_{j+\frac{1}{2}\downarrow}^\dagger \hat{c}_{j-\frac{1}{2}\uparrow} + \hat{c}_{-j+\frac{1}{2}\downarrow}^\dagger \hat{c}_{-j-\frac{1}{2}\uparrow} \right) + \text{H.c.} \right] \quad (4)$$

where λ_m^z is real and $\lambda_0^z = 0$ by Eq. (2b), $N = 2L + 1$ implying $L \in \mathbb{Z}$, $\hat{c}_{k\sigma}^\dagger$ creates an electron in the state $|k; \sigma\rangle$, which transforms according to the representation $\bar{\Gamma}_{k+\sigma}$, and sums in subscripts are defined modularly on the half-odd-integers $(-N/2, N/2]$.

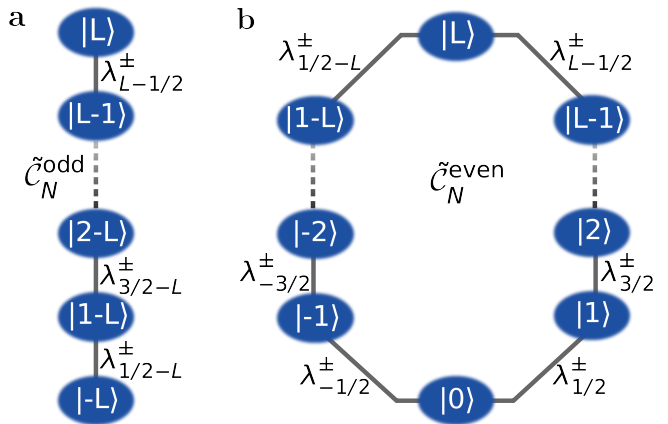


FIG. 1: Allowed matrix elements of H_{SO} for systems with cyclic symmetry, C_N . (a) For odd N there is a maximum (minimum) molecular angular momentum state $|L\rangle$ ($|-L\rangle$) that cannot be raised (lowered) by SMOC. For spherically symmetric systems (e.g., atoms) all shells contain an odd number of states, $2l + 1 = 1, 3, 5, \dots$ and have maximum (minimum) m_l values, thus the odd N cyclic and spherically symmetric cases are highly analogous. (b) In contrast, for even N all states couple to a state with equal total angular momentum about z , $j = k + \sigma$, e.g., $|L; \uparrow\rangle$ couples to $|1-L; \downarrow\rangle$.

Kramers’ theorem [via Eq. (2a)] implies that matrix elements between time reversed fermionic states vanish – importantly for odd N this includes $\langle -L; \downarrow | H_{\text{SO}} | L; \uparrow \rangle$ even though both $|-L; \downarrow\rangle$ and $|L; \uparrow\rangle$ transform according to $A_{N/2}$. Thus we find that, up to the values of matrix elements, which are not determined by symmetry, in the odd- N case the structure of Eq. (4) is equivalent to that in an atomic orbital with angular momentum L , where $H_{\text{SO}}^{\text{at}} = \lambda \mathbf{L} \cdot \mathbf{S}$. However, in general, the values of the constants break the SO(3) symmetry.

For even N the solutions of $L = (N-1)/2$ are half-odd-integers. However, if, instead, one defines $L = N/2$ for even N and applies the selection rules [Eqs. (2)] one again finds that the H_{SO} is given by Eq. (4), but now $\lambda_0^z = \lambda_L^z = 0$ by Eq. (2b). However, in the even case no λ_j^\pm vanish by symmetry. Thus, there are fundamental differences between odd- and even-membered rings, illustrated in Fig. 1. These are direct consequences of the modular addition, onto the interval $(-N/2, N/2]$, of angular momentum implicit in Eq. (2b).

The differences between odd- and even-membered rings can be understood by examining the character table (I). For even N the Born-von Kármán boundary conditions of the ring imply that a single state instantiates both the maximal and minimal molecular orbital angular momentum, $|L\rangle \equiv |-L\rangle$. In the language of signal processing, $|L\rangle$ and $|-L\rangle$ are aliases, see Fig. 2. Hence $|L; \uparrow\rangle$ and $|1-L; \downarrow\rangle \in \bar{E}_{(N-1)/2}$; similarly $|L; \downarrow\rangle$ and $|L-1; \uparrow\rangle \in \bar{E}_{(1-N)/2}$. That is, there is always more than one state with the maximal (minimal) total angular momentum, $j = k + \sigma$, and SMOC couples these states.

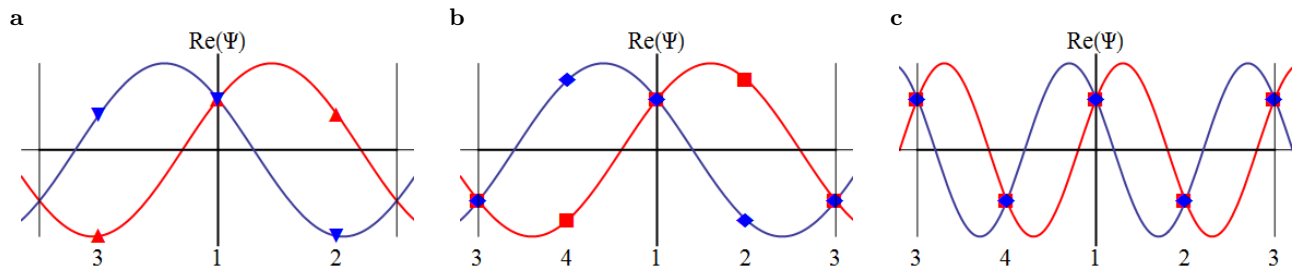


FIG. 2: Illustration of the aliasing of the maximum and minimum angular momentum states in even membered rings. Lines show the molecular orbital angular momentum states defined in Eq. (3) in the $N \rightarrow \infty$ limit. We plot snapshots of the real part of the wavefunction as it evolves under the trivial Schrödinger time evolution. Here we show the wavefunctions for $\omega_k t = 0.1$, where $\hbar\omega_k$ is the energy of the state $|k\rangle$. (a) For three sites the maximum ($k = +1$, red) and minimum ($k = -1$, blue) angular momentum states are distinguishable when sampled on the three sites (marked on the abscissa; values sampled are marked by triangles). (b) On four sites the $k = +1$ (red) and $k = -1$ (blue) angular momentum states remain distinguishable when sampled on the four sites (values sampled are marked by diamonds/squares). (c) However, the maximum ($k = +2$, red) and minimum ($k = -2$, blue) angular momentum states are *indistinguishable* when sampled on the four sites (values samples are marked by diamonds/squares); i.e., $|+2\rangle \equiv |-2\rangle$. For simplicity the phase factors, η_k , are not included in the figure, but, clearly, an overall phase factor cannot remove the aliasing. Animations of the full time evolution, shown in the Supplementary Information [45], underscore that this argument holds at all times.

This is highly analogous to umklapp scattering in crystals.

In contrast for odd N different states instantiate the maximal ($|L; \uparrow\rangle$) and minimal ($|-L; \downarrow\rangle$) *total* angular momenta. Both of these states transform as $A_{N/2}$ and they form a Kramers' doublet. Therefore, time reversal symmetric terms in the Hamiltonian (such as SOC) cannot cause an interaction between $|L; \uparrow\rangle$ and $|-L; \downarrow\rangle$; this would lift their degeneracy, violating Kramers' theorem [Eq. (2a)]. Thus the combination of \mathcal{C}_N symmetry and time reversal symmetry leads directly to the close analogy with atomic SOC in the odd N case.

In real space the SMOC takes the same form for both odd and even N :

$$H_{\text{SO}} = \sum_{r\sigma} \sigma \lambda_{rs}^z \hat{a}_{r\sigma}^\dagger \hat{a}_{s\sigma} + \frac{1}{2} \sum_{rs} \left[\lambda_{rs}^\pm \hat{a}_{r\downarrow}^\dagger \hat{a}_{s\uparrow} + \text{H.c.} \right], \quad (5)$$

where

$$\lambda_{rs}^z = \frac{2i}{N} \sum_{k=1}^L \lambda_k^z \sin[\phi k(r-s)],$$

$$\lambda_{rs}^\pm = -\frac{2}{N} \sum_{j=1/2}^{L-1/2} \lambda_j^\pm \sin[\phi j(r-s)] e^{i\phi(r+s)/2}$$

$$\text{and } \hat{a}_{r\sigma} = \frac{1}{\sqrt{N}} \sum_k e^{i\phi kr} \eta_k \hat{c}_{k\sigma}.$$

III. FIRST PRINCIPLES CALCULATIONS

The above arguments, based on symmetry considerations, only show that the SMOC is allowed. Therefore, it is natural to ask how large this effect is in real materials. Most of the multi-nuclear complexes synthesized

to date with strong intermolecular coupling have not included heavy atoms. $\text{Mo}_3\text{S}_7(\text{dmit})_3$ is a typical example [4, 6]. In the absence of SOC its low-energy electronic structure is described by three Wannier orbitals per spin per molecule. [36] We solved the four-component Dirac-Kohn-Sham equation in an all-electron full-potential local orbital basis using the FPLO package [38, 39]. The density was converged on a $(8 \times 8 \times 8)$ k -mesh using the Perdew-Burke-Ernzerhof exchange-correlation functional [40]. Localized Wannier [41] spinors were constructed from the twelve bands closest to the Fermi energy, corresponding to six spinors (three Kramers pairs) per molecule. We calculated the overlaps between Wannier spinors constructed from the solution of the four-component Dirac-Kohn-Sham equation within the same molecule to construct a first principles single particle effective low-energy Hamiltonian.

In addition to tight-binding terms found in one-component calculations [36], we find additional intramolecular SOC terms of precisely the form given in Eq. (5). Despite the relatively small atomic numbers of the constituent atoms the SMOC in $\text{Mo}_3\text{S}_7(\text{dmit})_3$ is significant: $\lambda^z \simeq 0.2t_c$, where t_c is the largest intermolecular hopping integral. [36] We also find significant anisotropy in the SMOC in $\text{Mo}_3\text{S}_7(\text{dmit})_3$: $\lambda^z/\lambda^\pm \simeq 2$. The Wannier spinor (Fig. 3) has significant weight on the Mo atoms in the core and S atoms in the dmit ligands. This suggests substituting either, or both, of these for heavier atoms, e.g., W or Se, could significantly increase the relative strength of the SMOC.

To investigate the effects of heavier metals we considered $[\text{W}_3\text{O}(\text{CCH}_3)(\text{O}_2\text{CCH}_3)_6(\text{H}_2\text{O})_3]$, which has a very similar electronic structure to $\text{Mo}_3\text{S}_7(\text{dmit})_3$ [37]. However, the hopping between $[\text{W}_3\text{O}(\text{CCH}_3)(\text{O}_2\text{CCH}_3)_6(\text{H}_2\text{O})_3]$ complexes is much weaker than that between $\text{Mo}_3\text{S}_7(\text{dmit})_3$ complexes;

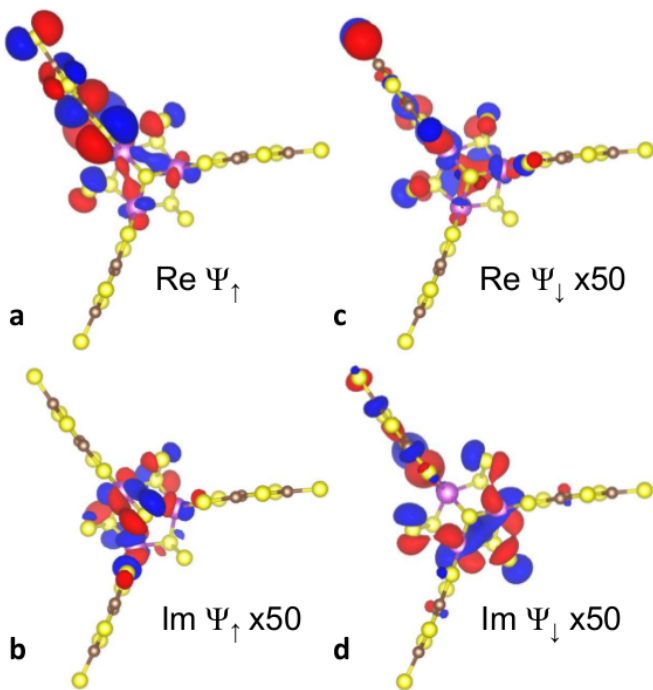


FIG. 3: The low energy physics of a single $\text{Mo}_3\text{S}_7(\text{dmit})_3$ molecule can be understood in terms of six Wannier spinors (three Kramers pairs). The large components of one is shown above; the others are related by the \tilde{C}_3 and/or time reversal symmetry. The four panels display the (a) real and (b) imaginary parts of the spin-up large component and the (c) real and (d) imaginary parts of the spin-down large component. Note that the isosurface in panel (a) corresponds to a contour value fifty times smaller than those in panels (b-d).

thus the band structure based approach, employed for $\text{Mo}_3\text{S}_7(\text{dmit})_3$, is impractical. We therefore calculated the electronic structure of a single complex both with and without SOC. These calculations were performed in a triple zeta plus polarization basis of Slater orbitals with the B3LYP functional [42] using the ADF package [43]. We then fit the parameters of the three site tight-binding model, with SMOC included in the second calculation, so as to reproduce the calculated frontier molecule orbital energies in both calculations. Again the SOC displays significantly anisotropy, however in this complex the largest SOC constant $\lambda^\pm \simeq 0.9t_c$, which is comparable to the iridates [11, 21].

IV. INTERPLAY OF MOLECULAR SPIN-ORBITAL COUPLING AND ELECTRONIC CORRELATIONS

To examine the effects of SMOC in cyclic molecules with strong electronic correlations we analyzed the simplest example: the t - J model for C_2 molecules with two orbitals per molecule. The Hamiltonian describing the

j th molecule is

$$H_{tJ} = P_0 \left[\sum_{\sigma} \left(t_c \hat{a}_{j1\sigma}^\dagger \hat{a}_{j2\sigma} + i\lambda \hat{a}_{j1\bar{\sigma}}^\dagger a_{j2\sigma} + H.c. \right) + J_c \left(\hat{\mathbf{S}}_{j1} \cdot \hat{\mathbf{S}}_{j2} - \frac{\hat{n}_{j1} \hat{n}_{j2}}{4} \right) \right] P_0, \quad (6)$$

where $\hat{\mathbf{S}}_{j\mu}$ ($\hat{n}_{j\mu}$) is the spin (number) operator for the μ th orbital on the j th molecule and P_0 projects out states that contain empty orbitals. The C_2 symmetry of the molecule implies that all $\lambda_k^z = 0$ and $\lambda = -2i\lambda_{1/2}^\pm \in \mathbb{R}$.

If neighboring molecules are related by inversion then λ is the same on both molecules. However, if they are related by a π rotation about the z -axis, λ must be of equal magnitude but opposite sign on the two molecules. For simplicity, we assume λ has the same magnitude on all molecules and consider arbitrary orientations of the molecules. We include t - J interactions between molecules: $P_0 \sum_{\langle ij\mu\nu \rangle \sigma} [t(\hat{a}_{i\mu\sigma}^\dagger \hat{a}_{j\nu\sigma} + H.c.) + J(\hat{\mathbf{S}}_{i\mu} \cdot \hat{\mathbf{S}}_{j\nu} - \hat{n}_{j1} \hat{n}_{j2}/4)] P_0$, where the angled brackets imply that the sum runs only over nearest neighbor orbitals, cf. Fig. 4a. We consider a ground state with one hole per molecule and assume that we are in a parameter regime consistent with a bulk molecular Mott insulator [26, 27]. The effective interactions between neighboring were evaluated analytically using the DiracQ package [44] in Mathematica. To second order in t (and hence first order in J) one finds a low-energy effective Hamiltonian describing pseudospin-1/2 degrees of freedom, $\hat{\mathbf{S}}_j = (\hat{\mathbf{S}}_j^x, \hat{\mathbf{S}}_j^y, \hat{\mathbf{S}}_j^z)$, on each molecule:

$$\mathcal{H}_{\text{eff}}^\pm = \sum_{ij\alpha\beta} \mathcal{J}_{\alpha\beta} \hat{\mathbf{S}}_i^\alpha \hat{\mathbf{S}}_j^\beta + \sum_{ij} \mathbf{D}^\pm \cdot \hat{\mathbf{S}}_i \times \hat{\mathbf{S}}_j + \varepsilon_0, \quad (7)$$

where \pm indicates the relative signs of λ on the two molecules. The exchange, $\mathcal{J}_{\alpha\beta}$, and Dzyaloshinskii-Moriya coupling, \mathbf{D}^\pm , are both strongly dependent on the relative orientation of the molecules. $\mathcal{J}_{\alpha\beta}$ is highly anisotropic, cf. Fig. 4, and independent of the relative signs of λ .

Hence, the SMOC leads to anisotropic exchange interactions. Furthermore, the anisotropy is strongly dependent on the relative orientation of the molecules. Thus it is possible to vary the exchange anisotropies between distinct pairs of molecules by arranging them in packing motifs with different angles between the pairs, cf. Fig. 4. This would open the way to providing new realizations of compass models, such as the Kitaev model [17, 18]. The inclusion of 5d metals opens up the possibility of reaching large effective SMOCs ($\lambda/t_c \sim 1$) in molecular crystals, as found in $\text{W}_3\text{O}(\text{CCH}_3)(\text{O}_2\text{CCH}_3)_6(\text{H}_2\text{O})_3$.

V. CONCLUSIONS

Thus, we have seen that in systems with cyclic symmetry the SOC is modified from the usual spherically

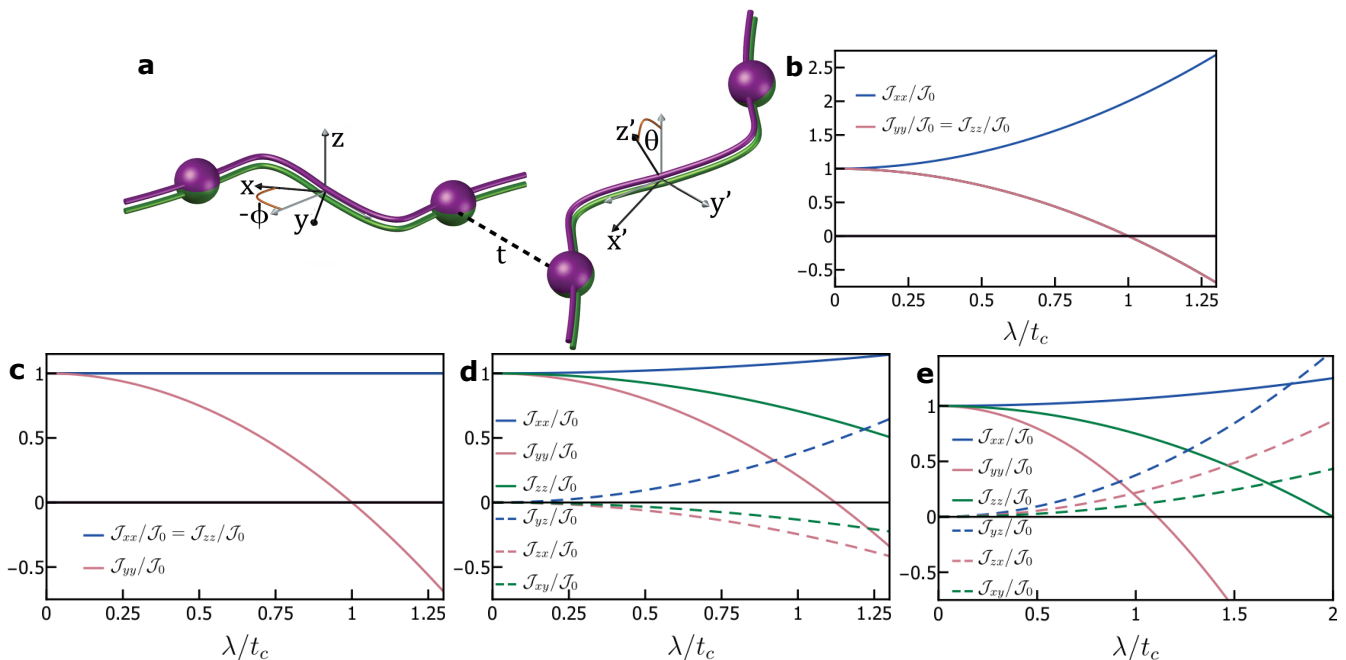


FIG. 4: The exchange anisotropies vary significantly in molecular materials with different packing motifs. (a) Sketch of a pair of nearest neighbors in the t - J model for C_2 molecules. Spheres indicate the Wannier orbitals and the curves connecting them show the molecular symmetry. The nearest neighbor intermolecular hopping, t , is marked. The local x and y axes are uniquely determined by the SMOC via the phase convention chosen in Eq. (3). Thus we parametrize the packing motif by the angles between the local axes on neighboring molecules: θ (ϕ) is the relative rotation about the y (z) axes; the effective Hamiltonian is independent of rotations about the x -axes. The local coordinate system is shown in black and the angles are marked relative to the gray axes, which are point in the same directions on both molecules. As we only consider pairwise interactions we write the effective Hamiltonian in the local coordinates of the i th molecule, cf. Eq. (7). (b) Parallel stacking ($\theta = \phi = 0$) leads to Ising anisotropy. (c) Perpendicular packing ($\theta = \pi/2$, $\phi = 0$) gives XY anisotropy. (d,e) More complicated packing gives greater anisotropy [here we plot (d) $\theta = \phi = 1$ and (e) $\phi = -\theta = 2\pi/3$]. In all plots $J = 0$ and $\mathcal{J}_0 = t^2 t_c^2 J_c / \{2[t_c^2 + \lambda^2][2(t_c^2 + \lambda^2) - J_c \sqrt{t_c^2 + \lambda^2}]\}$. Analytical expressions for $\mathcal{J}_{\alpha\beta}$ and \mathbf{D}^\pm are given in Appendix B.

symmetric case. In particular the spin couples to currents flowing around the molecule, rather than to intra-atomic angular momentum. For odd N time reversal symmetry forbids umklapp like spin-orbit scattering raising or lowering the molecular angular momentum across the Brillouin zone boundary. However, even N all molecular angular momentum states can be raised and lowered – this is a direct consequence of the the maximum and minimum molecular angular momenta being aliases for a single state.

Density functional calculations demonstrate that the coupling of spin to molecular orbital angular momenta is large in suitable multi-nuclear organometallic complexes. However, we stress that our results are not limited to these materials; and apply to all systems with appropriate symmetry.

We have discussed the consequences of this SMOC for exchange anisotropy in materials with strong electronic correlations. However, given the diverse implications of SOC for the low-energy behavior of materials containing heavy metals, the ideas presented above have potential applications ranging from organic light-emitting diodes to spintronics [1, 2, 7].

Acknowledgments

We thank Tom Stace and Xiuwen Zhou for helpful conversations. This work was supported by the Australian Research Council through grants FT130100161, DP130100757, DP160100060 and LE120100181. J.M. acknowledges financial support from (MAT2015-66128-R) MINECO/FEDER, UE. Density functional calculations were performed with resources from the National Computational Infrastructure (NCI), which is supported by the Australian Government.

Appendix A: Derivation of the selection rules [Eqs. (2)]

H_{SO} , like all Hamiltonian elements, belongs to the trivial representation A_0 ; it follows immediately from the \tilde{C}_N multiplication tables that

$$\langle \bar{j}_\mu | H_{\text{SO}} | \bar{i}_\nu \rangle = \Lambda_{j;\mu\nu} \delta_{ij}, \quad (\text{A1})$$

where $\Lambda_{j;\mu\nu}$ is a constant. Thus, H_{SO} conserves j .

Time reversal symmetry implies that $H_{\text{SO}} = \mathcal{T}^{-1}H_{\text{SO}}\mathcal{T}$. For fermionic representations $\mathcal{T}^2|\bar{j}_\mu\rangle = -|\bar{j}_\mu\rangle$. Thus, the antiunitarity of \mathcal{T} implies that

$$\langle \bar{j}_\mu | H_{\text{SO}} \mathcal{T} | \bar{i}_\nu \rangle = -\langle \bar{i}_\nu | H_{\text{SO}} \mathcal{T} | \bar{j}_\mu \rangle. \quad (\text{A2})$$

Setting $|\bar{j}_\mu\rangle = |\bar{i}_\nu\rangle$ yields Eq. (2a).

Further progress can be made by noting the explicit form of H_{SO} , Eq. (1). In particular, σ acts only on the spin subspace whereas \mathbf{K} acts only on the molecular orbital subspace. K^z , K^+ , and K^- transform according to A_0 , E_1 , and E_{-1} respectively for $N \geq 3$. Thus,

$$\begin{aligned} \langle \underline{k}_\mu; \sigma | H_{\text{SO}} | \underline{q}_\nu; \sigma \rangle &= \langle \underline{k}_\mu | \mathbf{K} | \underline{q}_\nu \rangle \cdot \langle \sigma | \sigma \rangle \\ &= \sigma \langle \underline{k}_\mu | K^z | \underline{q}_\nu \rangle = \sigma \lambda_{k;\mu\nu}^z \delta_{kq}. \end{aligned} \quad (\text{A3})$$

It is straightforward to show that the same result also holds for $N = 1, 2$. Time reversal symmetry requires that

$$\langle \bar{j}_\mu | H_{\text{SO}} | \bar{i}_\nu \rangle = (-1)^{i+j-1} \langle \overline{-i}_\nu | H_{\text{SO}} | \overline{-j}_\mu \rangle. \quad (\text{A4})$$

Considering $i = j$ and noting that both are half-odd integers yields $\lambda_{k;\mu\nu}^z = (\lambda_{k;\nu\mu}^z)^* = -\lambda_{-k;\mu\nu}^z$. Hence $\lambda_{k;\mu\mu}^z \in \mathbb{R}$, which completes the proof of Eq. (2b).

As Γ_k is a bosonic representation, Eq. (A3) and the orthogonality of the basis functions imply that if $\mathcal{T}|\underline{k}_\mu\rangle = |\underline{k}_\mu\rangle$ then $\lambda_{k;\mu\nu}^z = 0$ for all μ, ν . Thus $\lambda_{0;\mu\nu}^z = 0$ for all N and $\lambda_{N/2;\mu\nu}^z = 0$ for even N .

Equation (2c) follows similarly on noting that

$$\langle \underline{q}_\nu; \downarrow | H_{\text{SO}} | \underline{k}_\mu; \uparrow \rangle = \langle \underline{q}_\nu | K^+ | \underline{k}_\mu \rangle \in \Gamma_{-q} \otimes E_1 \otimes \Gamma_k = A_0 \quad (\text{A5})$$

if and only if $k = q - 1$. And that

$$\langle \underline{q}_\nu; \uparrow | H_{\text{SO}} | \underline{k}_\mu; \downarrow \rangle = \langle \underline{q}_\nu | K^- | \underline{k}_\mu \rangle \in \Gamma_{-q} \otimes E_{-1} \otimes \Gamma_k = A_0 \quad (\text{A6})$$

if and only if $k = q + 1$.

Appendix B: Magnetic interactions

The parameters for equation (6) are

$$\begin{aligned} \mathcal{J}_{\beta\alpha} &= \mathcal{J}_{\alpha\beta}, \\ \mathcal{J}_{xx} &= \mathcal{J}_0 [1 + \Lambda^2 \cos^2 \theta \cos^2 \phi] + \frac{J}{4}, \\ \mathcal{J}_{yy} &= \mathcal{J}_0 \{1 - \Lambda^2 [1 + (\cos^2 \phi - 1) \cos^2 \theta]\} + \frac{J}{4}, \\ \mathcal{J}_{zz} &= \mathcal{J}_0 [1 - \Lambda^2 \cos^2 \theta] + \frac{J}{4}, \\ \mathcal{J}_{xy} &= -\mathcal{J}_0 \Lambda^2 \cos^2 \theta \cos \phi \sin \phi, \\ \mathcal{J}_{zx} &= -\mathcal{J}_0 \Lambda^2 \cos \theta \sin \theta \cos \phi, \\ \mathcal{J}_{yz} &= \mathcal{J}_0 \Lambda^2 \cos \theta \sin \theta \sin \phi, \\ D_y^\pm &= \mathcal{J}_0 \Lambda \cos \theta \sin \phi, \\ D_z^\pm &= \mathcal{J}_0 \Lambda \sin \theta \\ \varepsilon_0 &= -\frac{\mathcal{J}_0}{4J_c} (1 + \Lambda^2) \left[8\sqrt{t_c^2(1 + \Lambda^2)} - 3J_c \right] - \frac{J}{16}, \end{aligned}$$

where $\Lambda = \lambda/t_c$ and

$$\mathcal{J}_0 = \frac{t^2 t_c^2 J_c}{2(t_c^2 + \lambda^2) \left[2(t_c^2 + \lambda^2) - J_c \sqrt{(t_c^2 + \lambda^2)} \right]}.$$

These parameters are the same regardless of the relative signs of λ ; however,

$$D_x^\pm = \mathcal{J}_0 \Lambda (\pm 1 - \cos \theta \cos \phi)$$

is not. In the above ϕ is the angle between the local z -axes of the molecules and θ is the angle between the local y -axes of the molecules. Relative rotation about the x -axis does not change the effective Hamiltonian. The local x and y axes are uniquely determined by the SOC via the phase convention chosen in equation (3).

-
- [1] A. Manchon, H. C. Koo, J. Nitta, S. M. Frolov, and R. A. Duine, *New perspectives for Rashba spinorbit coupling*, Nature Materials **14**, 871882 (2015)
- [2] G. Bihlmayer, O. Rader, and R. Winkler, *Focus on the Rashba effect*, New J. Phys. **17** 050202 (2015).
- [3] J. J. Sakurai and J. J. Napolitano *Modern Quantum Mechanics* (Pearson, Harlow, 2014).
- [4] R. Llugar and C. Vicent, *Trinuclear molybdenum cluster sulfides coordinated to dithiolene ligands and their use in the development of molecular conductors*, Coord. Chem. Rev. **254**, 1534-1548 (2010).
- [5] D. Belo and M. Almeida, *Transition metal complexes based on thiophene-dithiolene ligands*, Coord. Chem. Rev. **254**, 1479-1492 (2010).
- [6] R. Llugar *et al.* *Single-Component Magnetic Conductors Based on Mo₃S₇ Trinuclear Clusters with Outer Dithiolate Ligands*, J. Am. Chem. Soc. **126**, 12076-12083. (2004).
- [7] B. J. Powell, *Theories of phosphorescence in organo-transition metal complexes From relativistic effects to simple models and design principles for organic light-emitting diodes*, Coord. Chem. Rev. **295**, 46 (2015).
- [8] X.-L. Qi and S.-C. Zhang, *Topological insulators and superconductors*, Rev. Mod. Phys., **83**, 1057-1110 (2011).
- [9] S.-Y. Xu *et al.* *Discovery of a Weyl Fermion semimetal and topological Fermi arcs*, Science, **349**, 613-617 (2015).
- [10] X. Wan, A. M. Turner, A. Vishwanath and S. Y. Savrasov, *Topological semimetal and Fermi-arc surface states in the electronic structure of pyrochlore iridates*, Phys. Rev. B, **83**, 205101 (2011).
- [11] W. Witczak-Krempa, G. Chen, Y. B. Kim and L. Balents, *Correlated Quantum Phenomena in the Strong*

- Spin-Orbit Regime*, Annu. Rev. Condens. Matter Phys. **5**, 57-82 (2014).
- [12] A. A. Soluyanov, D. Gresch, Z. Wang, Q. Wu, M. Troyer, X. Dai and B. A. Bernevig, *Type-II Weyl semimetals*, Nature **527**, 495-498 (2015).
- [13] D. Pesin and L. Balents, *Mott physics and band topology in materials with strong spin-orbit interaction*, Nat. Phys. **6**, 376-381 (2010).
- [14] M. Dzero, K. Sun, V. Galitski and P. Coleman, *Topological Kondo Insulators*, Phys. Rev. Lett. **104**, 106408 (2010).
- [15] X. Chen, Z.-C. Gu and X.-G. Wen, *Local unitary transformation, long-range quantum entanglement, wave function renormalization, and topological order*, Phys. Rev. B **82**, 155138 (2010).
- [16] C. Castelnovo, R. Moessner and S. L. Sondhi, *Spin Ice, Fractionalization, and Topological Order*, Annu. Rev. Condens. Matter Phys. **3**, 3555 (2012).
- [17] A. Kitaev, *Anyons in an exactly solved model and beyond*, Ann. Phys. **321**, 2-111 (2006).
- [18] Z. Nussinov and J. van den Brink, *Compass models: Theory and physical motivations*, Rev. Mod. Phys. **87**, 1 (2015).
- [19] J. K. Pachos, *Introduction to Topological Quantum Computation* (Cambridge University Press, Cambridge, 2012).
- [20] G. Jackeli and G. Khaliullin, *Mott Insulators in the Strong Spin-Orbit Coupling Limit: From Heisenberg to a Quantum Compass and Kitaev Models*, Phys. Rev. Lett. **102**, 017205 (2009).
- [21] J. G. Rau, E. K.-H. Lee and H.-Y. Kee, *Spin-Orbit Physics Giving Rise to Novel Phases in Correlated Systems: Iridates and Related Materials*, Annu. Rev. Condens. Matter Phys. **7**, 195-221 (2016).
- [22] I. I. Mazin, H. O. Jeschke, K. Foyevtsova, R. Valentí, and D. I. Khomskii, *Na_2IrO_3 as a Molecular Orbital Crystal*, Phys. Rev. Lett. **109**, 197201 (2012).
- [23] Pedersen, K. S. *et al.* *Iridates from the molecular side*, Nat. Commun. **7**, 12195 (2016).
- [24] M. G. Yamada, H. Fujita, and M. Oshikawa, *Designing Kitaev spin liquids in metal-organic framework*, arXiv:1605.04471.
- [25] A. Abragam and B. Bleaney, *Electron paramagnetic resonance of transition ions* (Clarendon Press, Oxford, 1970).
- [26] K. Kanoda and R. Kato, *Mott Physics in Organic Conductors with Triangular Lattices*, Annu. Rev. Condens. Matter Phys. **2**, 167-188 (2011).
- [27] B. J. Powell and R. H. McKenzie, *Strong electronic correlations in superconducting organic charge transfer salt*, J. Phys.: Condens. Matter **18**, R827-R826 (2006).
- [28] S. M. Winter, S. Hill and R. T. Oakley, *Magnetic Ordering and Anisotropy in Heavy Atom Radicals*, J. Am. Chem. Soc. **137**, 3720-3730 (2015).
- [29] K. M. Dyall and K. Færi, *Introduction to Relativistic Quantum Chemistry* (Oxford University Press, New York, 2007).
- [30] H. Min, *et al.* *Intrinsic and Rashba spin-orbit interactions in graphene sheets*, Phys. Rev. B **74**, 165310 (2006).
- [31] D. Huertas-Hernando, F. Guinea and A. Brataas, *Spin-orbit coupling in curved graphene, fullerenes, nanotubes, and nanotube caps*, Phys. Rev. B **74**, 155426 (2006).
- [32] G. F. Koster, J. O. Dimmock, R. G. Wheeler and H. Statz, *Properties of the Thirty-two Point Groups* (MIT press, Cambridge, 1963).
- [33] M. S. Dresselhaus, G. Dresselhaus and A. Jorio, *Group Theory* (Springer, Berlin, 2008).
- [34] B. A. Hess, C. M. Marian, U. Wahlgren and O. Gropen, *A mean-field spin-orbit method applicable to correlated wavefunctions*, Chem. Phys. Lett. **251**, 365-371 (1996).
- [35] F. Neese, *Efficient and accurate approximations to the molecular spin-orbit coupling operator and their use in molecular g-tensor calculations*, J. Chem. Phys. **122**, 034107 (2005).
- [36] A. C. Jacko, C. Janani, K. Koepernik, and B. J. Powell, *Emergence of quasi-one-dimensional physics in a nearly-isotropic three-dimensional molecular crystal: Ab initio modeling of $\text{Mo}_3\text{S}_7(\text{dmit})_3$* , Phys. Rev. B **91**, 125140 (2015).
- [37] F. A. Cotton, Z. Dori, M. Kapon, D. O. Marler, G. M. Reisner, W. Schwotzer, and M. Shaii, *The First Alkylidyne-Capped Tritungsten(IV) Cluster Compounds: Preparation, Structure, and Properties of $[\text{W}_3\text{O}(\text{CCH}_3)(\text{O}_2\text{CCH}_3)_6(\text{H}_2\text{O})_3]\text{Br}_2 \cdot 2\text{H}_2\text{O}$* , Inorg. Chem. **24**, 4381-4384 (1985).
- [38] K. Koepernik and H. Eschrig, *Full-potential nonorthogonal local-orbital minimum-basis band-structure scheme*, Phys. Rev. B **59**, 1743-1757 (1999).
- [39] H. Eschrig, M. Richter and I. Opahle, "chap. 12: Relativistic solid state calculations", in *Theoretical and Computational Chemistry*, edited by P. Schwerdtfeger (2004), pp. 723-776.
- [40] J. P. Perdew, K. Burke and M. Ernzerhof, *Generalized gradient approximation made simple*, Phys. Rev. Lett. **77**, 3865-3868 (1996).
- [41] N., Marzari, A. A. Mostofi, J. R. Yates, I. Souza and D. Vanderbilt, *Maximally localized Wannier functions: Theory and applications*, Rev. Mod. Phys. **84**, 1419-1475 (2012).
- [42] A. D. Becke, *Density-functional thermochemistry. III. The role of exact exchange*, J. Chem. Phys. **98**, 5648-5652 (1993).
- [43] G. te Velde, F. M. Bickelhaupt, E. J. Baerends, C. Fonseca Guerra, S. J. A. van Gisbergen, J. G. Snijders and T. Ziegler, *Chemistry with ADF*, J. Comp. Chem. **22** 931967 (2001).
- [44] J. G. Wright and B. S. Shastry, arXiv:1301.4494 (2013).
- [45] Animated versions of Figs. 2a-c can be viewed at <https://youtu.be/hh0A59aKHoo>, <https://youtu.be/LGLPkQzcQ9o>, and <https://youtu.be/oAW03j408Vw> respectively.